Electronic Research Archive

https://www.aimspress.com/journal/era

ERA, 34(6): 3945–3967.
DOI: 10.3934/era.2026177
Received: 04 April 2026
Revised: 26 April 2026
Accepted: 30 April 2026
Published: 13 May 2026

Research article

Finite difference scheme on non-uniform meshes for third-kind Volterra integral equations with nonsmooth solutions and its error analysis

Jiaxu Liang[1], **Ruiqi Yu**[1], **Yu Li**[1] **and Yan Fan**[2,*]

[1] Department of Mathematics, Northeast Forestry University, Harbin 150040, China
[2] Xingzhi College, Zhejiang Normal University, Jinhua 321004, China

* **Correspondence:** Email: fanyan@zjnu.edu.cn.

Abstract: This paper presents a high-order numerical method for nonlinear Volterra integral equations of the third kind (VIE3) with weakly singular kernels. To overcome the accuracy loss caused by the unbounded derivatives of the solution near the origin, we propose a fractional Adams-Simpson-type method on a graded mesh. The stability and convergence of the proposed scheme, along with detailed error estimates, are rigorously established. It is shown that the method achieves an optimal convergence order of $4 - \alpha - \lambda\beta$, provided the mesh grading exponent λ is chosen appropriately. Numerical experiments are presented to validate the theoretical convergence results and to demonstrate the effectiveness of the method in resolving initial singularities.

Keywords: Volterra integral equation of the third kind; weakly singular; Adams-Simpson-type scheme; non-uniform meshes

1. Introduction

In this paper, we consider the Volterra integral equation of the third kind (VIE3) as follows:

$$t^{\beta}u(t) = f(t) + \int_0^t (t-s)^{-\alpha} K(t,s)\, u(s)\, \mathrm{d}s, \quad t \in \mathrm{I} = [0,T], \tag{1.1}$$

with the initial condition $u(0) = u_0$, where $\alpha \in [0,1)$, $\beta \in (0,+\infty)$, $f(\cdot)$ is a continuous function on the interval I, and $u(\cdot)$ is an unknown function. The given continuous function $K(\cdot,\cdot)$ is defined on $D = \{(t,s) : 0 \le s \le t \le T\}$.

Theoretical and numerical studies of Volterra integral equations have received sustained attention in recent years. Early works focused on the existence and regularity of analytic solutions: e.g., Allaei et al. [1] established the existence, uniqueness, and regularity theory of solutions for Volterra integral equations containing weakly singular kernels coupled with smooth kernels. Gennadi Vainikko

proposed the transformation conditions for transforming them into cordial Volterra integral equations [2, 3]. Meanwhile, it is shown that the regularity of solutions is closely related to the singularity of the kernel function and the type of equations [4]. Even if the input function is sufficiently smooth, the derivative order of the solution is still limited by the singularity exponent of the kernel function α, which needs to be compensated by the theory of non-uniform grids or weighted spaces.

Time-fractional differential equations are known to exhibit solution singularities at the initial time that are closely related to those arising in VIE3. Consequently, numerical techniques developed for handling singularities in time-fractional differential equations can be adapted to the numerical solution of weakly singular Volterra integral equations. The development of such numerical methods can be traced back to the foundational work of Lubich, who introduced fractional linear multistep methods based on convolution quadrature for weakly singular Volterra integral equations of the second kind [5, 6]. Subsequently, the stability analysis of convolution quadrature methods was established [7]. In parallel, Diethelm et al. developed an Adams-type predictor-corrector method for time fractional differential equations [8, 9], which was later refined by Li and Tao [10] and further improved by Yan et al. [11] with a segmented quadratic interpolation technique.

However, the weak singularity at the initial moment is still the bottleneck of the numerical method. Fractional order integral approximation techniques effectively solve the difficulty of accuracy decay near the singularity by introducing special weighting functions and integral transformation strategies when dealing with the weak singular kernel problem of the Volterra integral equation. However, the introduction of weighting functions usually requires additional integral transformation steps, leading to an increase in algorithmic complexity. As a result, non-uniform grid compensation strategies have been widely adopted. Liu et al. [12, 13] analyzed the error characteristics of fractional rectangular, trapezoidal, and predictive correction methods on hierarchical grids and extended Adams' method to singular problems. Lyu and Vong [14] combined segmented quadratic interpolation with hierarchical grids to achieve a higher-order approximation. The present work focuses on equations with a constant singularity exponent α. Another important class of problems involves variable-exponent kernels, where $\alpha = \alpha(t)$. For example, Zheng [15] presented a general framework for analyzing such models.

This paper aims to construct a class of efficient high-order Adams-Simpson-type methods for the VIE3 (1.1). First, we introduce a generalized non-uniform grid, building on the concept of a non-uniform grid that covers special hierarchical grid cases, to handle the initial singularity. Next, we reconstruct the piecewise quadratic interpolation process to reduce the computational complexity within the block discrete framework. Finally, we analyze the error of the proposed method under the non-uniform grid. The remainder of this paper is organized as follows. In Section 2, the fractional Adams-Simpson-type numerical scheme is derived using the Lagrange interpolation method. In Section 3, we construct a non-uniform grid and analyze the local truncation error of the proposed numerical method. The convergence and stability of the method are also studied via a modified fractional Grönwall inequality. Several numerical experiments are provided in Section 4 to demonstrate the high-order accuracy of the numerical method. Section 5 concludes the paper and discusses future research prospects.

2. Construction of the fractional Adams-Simpson-type scheme

The existence, uniqueness, and regularity properties of solutions to (1.1) for $\alpha \in (0,1)$ and $\beta > 1$ have been studied in [1]. When $\beta = 1$, a unique continuous solution exists if $K(0,0) < 1$. The case $K(0,0) \geq 1$ may lead to non-existence and non-uniqueness or require additional regularity conditions, depending on the kernel structure. For $0 < \beta < 1$, the equation admits a unique continuous solution under smooth kernel assumptions. For $\beta > 1$, the behavior of the solution depends critically on the kernel's structure, particularly when $K(t,x)$ takes the form $x^{\beta-1}h(t,x)$ with h continuous. In the weakly singular case $0 < \alpha < 1$, the interplay between α and β further refines solvability: The condition $\alpha+\beta < 1$ ensures a unique solution, while $\alpha+\beta \geq 1$ introduces more complicated singular behavior. In particular, when $\alpha+\beta > 1$, to facilitate the analysis of the solution's singularity structure, the kernel is often assumed to take the form $x^{\alpha+\beta-1}h(t,x)$ with h continuous. Under such assumptions, the solutions may exhibit a power-law structure $u(t) = t^{\sigma}v(t)$, where $\sigma \in (0,1)$ depends on α and β and $v(t)$ is at least continuous on $[0,T]$. This suggests that $u(t)$ behaves as Ct^{σ}, which was first strictly proved in [16].

Assumption 2.1. *Assume that the solutions $u(t)$ of VIE3 (1.1) lies in $C^4(0,T]$ and there exist a constant $C > 0$ such that*

$$\left|u^{(l)}(t)\right| \leq C\left(1 + t^{\sigma-l}\right), \quad t \in (0,T], \quad l = 0,1,2,3,4, \tag{2.1}$$

where $\sigma \in (0,1)$ is a real number and C may depend on σ but is independent of t.

Assumption 2.1 assumes a weakly singular behavior of u at $t = 0$. While u remains continuous, its derivatives $u^{(l)}$ $(l = 1,2,3,4)$ exhibit blow-up characteristics. The singular index σ is determined by the parameter coupling relationship of $\alpha+\beta$ and the specific form of the kernel. Specifically, when the kernel behaves as $x^{\beta-1}h(t,x)$, one typically has $\sigma = \beta - 1$; when the kernel takes the form $x^{\alpha+\beta-1}h(t,x)$, one has $\sigma = \alpha+\beta-1$. Thus, for a given equation, σ can be estimated a priori by examining the asymptotic behavior of $K(t,s)$ near $s = 0$. This can ensure that the initial singularity of the solution is controllable. When $\alpha = 0$, the kernel $(t-s)^{-\alpha}$ reduces to 1, and Eq (1.1) becomes a standard VIE3. In this paper, we will solely discuss the efficient numerical solutions for this type of VIE3 (1.1) with $\alpha \in [0,1)$. The numerical scheme and the theoretical analysis presented below remain valid for $\alpha = 0$. Throughout this paper, the symbol C denotes a generic positive constant that may take different values at different occurrences.

Next, we construct the fractional Adams-Simpson-type scheme. Let $C^{a+1}(0,T]$ denote the set of all continuous functions with their $(a+1)$-th derivatives also continuous on $(0,T]$. Let $0 = t_0 < t_1 < \cdots < t_N = T$ with $\tau_n = t_n - t_{n-1}$, $1 \leq n \leq N$ as the step length. Then, for any function u lying in $L_1[0,T] \cap C^{a+1}(0,T]$, the Lagrange interpolation polynomial of degree a for u relative to the nodes $t_b, t_{b-1}, \cdots, t_{b-a}$, with two given nonnegative integers $a, b \in \mathbb{N}$ satisfying $a \leq b$, is defined as

$$L_{0,b}u(t) = u(t_b), \quad L_{a,b}u(t) = \sum_{k=b-a}^{b} l_{k,a,b}(t)\, u(t_k), \quad a > 0,$$

where the coefficients $l_{k,a,b}(t)$ are

$$l_{k,a,b}(t) = \frac{\prod_{k^*=b-a,\ k^*\neq k}^{b}(t - t_{k^*})}{\prod_{k^*=b-a,\ k^*\neq k}^{b}(t_k - t_{k^*})}, \quad k = b-a, \ldots, b.$$

The corresponding interpolation error is represented by

$$R_{a,b}u(t) := u(t) - L_{a,b}u(t). \tag{2.2}$$

By standard Lagrange interpolation theory, if $u \in C^{a+1}(0,T]$, the remainder $R_{a,b}u(t)$ can be expressed in integral form involving $u^{(a+1)}$. The explicit expressions of $R_{a,b}u(t)$ used in the subsequent analysis will be given later.

For $n \geq 1$, taking $t = t_n$ in Eq (1.1), we get

$$t_n^{\beta}u(t_n) = f(t_n) + \int_0^{t_n} (t_n - s)^{-\alpha}K(t_n, s)\,u(s)\mathrm{d}s. \tag{2.3}$$

To approximate the above integral, we denote

$$ {}_0\hat{I}_t^{\alpha}u(t_1) = \int_{t_0}^{t_1} (t_1 - s)^{-\alpha}K(t_1, s)\,L_{0,0}u(s)\,\mathrm{d}s,$$

$$ {}_0\hat{I}_t^{\alpha}u(t_2) = \int_{t_0}^{t_2} (t_2 - s)^{-\alpha}K(t_2, s)\,L_{1,1}u(s)\,\mathrm{d}s.$$

When $n \geq 3$ and n is odd, let

$$ {}_0\hat{I}_t^{\alpha}u(t_n) = \sum_{k=0}^{\frac{n-3}{2}} \int_{t_{2k}}^{t_{2k+2}} (t_n - s)^{-\alpha}K(t_n, s)L_{2,2k+2}u(s)\,\mathrm{d}s + \int_{t_{n-1}}^{t_n} (t_n - s)^{-\alpha}K(t_n, s)L_{2,n-1}u(s)\,\mathrm{d}s.$$

When $n \geq 4$ and n is even, let

$$ {}_0\hat{I}_t^{\alpha}u(t_n) = \sum_{k=0}^{\frac{n-4}{2}} \int_{t_{2k}}^{t_{2k+2}} (t_n - s)^{-\alpha}K(t_n, s)L_{2,2k+2}u(s)\,\mathrm{d}s + \int_{t_{n-2}}^{t_n} (t_n - s)^{-\alpha}K(t_n, s)L_{2,n-1}u(s)\,\mathrm{d}s.$$

Then, we approximate the integral in (2.3) by

$$\int_0^{t_n} (t_n - s)^{-\alpha}K(t_n, s)\,u(s)\,\mathrm{d}s \approx {}_0\hat{I}_t^{\alpha}u(t_n), \quad 1 \leq n \leq N. \tag{2.4}$$

The quadrature error of this approximation will be analyzed in detail in the next section, where it is shown that the local truncation error achieves the order $\min\{\lambda(\sigma + 1 - \alpha), 4 - \alpha\}$ under the non-uniform grid assumptions.

For simplicity, we introduce the coefficients $q_{k,i,j}^{(\alpha)}$ defined as

$$q_{0,0,1}^{(\alpha)} = \int_{t_0}^{t_1} (t_1 - s)^{-\alpha}K(t_1, s)\,\mathrm{d}s,$$

$$q_{k,1,2}^{(\alpha)} = \int_{t_0}^{t_2} (t_2 - s)^{-\alpha}K(t_2, s)\,l_{k,1,1}(s)\,\mathrm{d}s, \quad k = 0, 1,$$

and for $k = n-3, n-2, n-1$ with $n \geq 3$, there is

$$q_{k,n-1,n}^{(\alpha)} = \begin{cases} \displaystyle\int_{t_{n-1}}^{t_n} (t_n - s)^{-\alpha}K(t_n, s)l_{k,2,n-1}(s)\mathrm{d}s, & n \text{ is odd}, \\ \displaystyle\int_{t_{n-2}}^{t_n} (t_n - s)^{-\alpha}K(t_n, s)l_{k,2,n-1}(s)\mathrm{d}s, & n \text{ is even}. \end{cases}$$

For $k = b-2, b-1, b$, $2 \le b \le n-1$, $n \ge 3$, we denote

$$p_{k,b,n}^{(\alpha)} = \int_{t_{b-2}}^{t_b} (t_n - s)^{-\alpha} K(t_n, s)\, l_{k,2,b}(s) \mathrm{d}s.$$

Note that $b \le n-1$, so $t_n - s > 0$ on $[t_{b-2}, t_b]$ and the integral is well defined. Then, the above expression can be rewritten as

$$\begin{aligned}
{}_0\hat{I}_t^{\alpha} u(t_1) &= \int_{t_0}^{t_1} (t_1 - s)^{-\alpha} K(t_1, s)\, u(t_0)\, \mathrm{d}s = q_{0,0,1}^{(\alpha)} u(t_0), \\
{}_0\hat{I}_t^{\alpha} u(t_2) &= \int_{t_0}^{t_2} (t_2 - s)^{-\alpha} K(t_2, s) \left(\sum_{k=0}^{1} l_{k,1,1}(s)\, u(t_k) \right) \mathrm{d}s = \sum_{k=0}^{1} q_{k,1,2}^{(\alpha)} u(t_k),
\end{aligned}$$

and for all odd integers not less than 3, it has

$$\begin{aligned}
{}_0\hat{I}_t^{\alpha} u(t_n) &= \sum_{k=0}^{\frac{n-3}{2}} \int_{t_{2k}}^{t_{2k+2}} \frac{K(t_n, s)}{(t_n - s)^{\alpha}} \left(\sum_{m=2k}^{2k+2} l_{m,2,2k+2}(s) u(t_m) \right) \mathrm{d}s + \int_{t_{n-1}}^{t_n} \frac{K(t_n, s)}{(t_n - s)^{\alpha}} \left(\sum_{k=n-3}^{n-1} l_{k,2,n-1}(s) u(t_k) \right) \mathrm{d}s \\
&= \sum_{k=0}^{\frac{n-3}{2}} \sum_{m=2k}^{2k+2} p_{m,2k+2,n}^{(\alpha)} u(t_m) + \sum_{k=n-3}^{n-1} q_{k,n-1,n}^{(\alpha)} u(t_k) \\
&= \sum_{k=0}^{\frac{n-3}{2}} p_{2k,2k+2,n}^{(\alpha)} u(t_{2k}) + \sum_{k=0}^{\frac{n-3}{2}} p_{2k+1,2k+2,n}^{(\alpha)} u(t_{2k+1}) + \sum_{k=0}^{\frac{n-3}{2}} p_{2k+2,2k+2,n}^{(\alpha)} u(t_{2k+2}) + \sum_{k=n-3}^{n-1} q_{k,n-1,n}^{(\alpha)} u(t_k).
\end{aligned}$$

For all even integers not less than 4, it gets

$$\begin{aligned}
{}_0\hat{I}_t^{\alpha} u(t_n) &= \sum_{k=0}^{\frac{n-4}{2}} \int_{t_{2k}}^{t_{2k+2}} \frac{K(t_n, s)}{(t_n - s)^{\alpha}} \left(\sum_{m=2k}^{2k+2} l_{m,2,2k+2}(s) u(t_m) \right) \mathrm{d}s + \int_{t_{n-2}}^{t_n} \frac{K(t_n, s)}{(t_n - s)^{\alpha}} \left(\sum_{k=n-3}^{n-1} l_{k,2,n-1}(s) u(t_k) \right) \mathrm{d}s \\
&= \sum_{k=0}^{\frac{n-4}{2}} \sum_{m=2k}^{2k+2} p_{m,2k+2,n}^{(\alpha)} u(t_m) + \sum_{k=n-3}^{n-1} q_{k,n-1,n}^{(\alpha)} u(t_k) \\
&= \sum_{k=0}^{\frac{n-4}{2}} p_{2k,2k+2,n}^{(\alpha)} u(t_{2k}) + \sum_{k=0}^{\frac{n-4}{2}} p_{2k+1,2k+2,n}^{(\alpha)} u(t_{2k+1}) + \sum_{k=0}^{\frac{n-4}{2}} p_{2k+2,2k+2,n}^{(\alpha)} u(t_{2k+2}) + \sum_{k=n-3}^{n-1} q_{k,n-1,n}^{(\alpha)} u(t_k).
\end{aligned}$$

Furthermore, we define

$$\begin{aligned}
&Q_{0,1}^{(\alpha)} = q_{0,0,1}^{(\alpha)}, \quad Q_{k,2}^{(\alpha)} = q_{k,1,2}^{(\alpha)} (k = 0, 1), \quad Q_{k,3}^{(\alpha)} = p_{k,2,3}^{(\alpha)} + q_{k,2,3}^{(\alpha)}, \quad k = 0, 1, 2, \\
&Q_{k,4}^{(\alpha)} = \begin{cases} p_{0,2,4}^{(\alpha)}, & k = 0, \\ p_{k,2,4}^{(\alpha)} + q_{k,3,4}^{(\alpha)}, & k = 1, 2, \\ q_{3,3,4}^{(\alpha)}, & k = 3, \end{cases} \quad Q_{k,5}^{(\alpha)} = \begin{cases} p_{k,2,5}^{(\alpha)}, & k = 0, 1, \\ p_{2,2,5}^{(\alpha)} + p_{2,4,5}^{(\alpha)} + q_{2,4,5}^{(\alpha)}, & k = 2, \\ p_{k,4,5}^{(\alpha)} + q_{k,4,5}^{(\alpha)}, & k = 3, 4, \end{cases} \\
&Q_{k,6}^{(\alpha)} = \begin{cases} p_{k,2,6}^{(\alpha)}, & k = 0, 1, \\ p_{2,2,6}^{(\alpha)} + p_{2,4,6}^{(\alpha)}, & k = 2, \\ p_{k,4,6}^{(\alpha)} + q_{k,5,6}^{(\alpha)}, & k = 3, 4, \\ q_{5,5,6}^{(\alpha)}, & k = 5. \end{cases}
\end{aligned}$$

When $n \geq 7$ and is odd, it is

$$Q_{k,n}^{(\alpha)} = \begin{cases} p_{0,2,n}^{(\alpha)}, & k = 0, \\ p_{2m+1,2m+2,n}^{(\alpha)}, & k = 2m+1, m = 0, 1, \cdots, \frac{n-5}{2}, \\ p_{2m,2m,n}^{(\alpha)} + p_{2m,2m+2,n}^{(\alpha)}, & k = 2m, m = 1, \cdots, \frac{n-5}{2}, \\ p_{n-3,n-3,n}^{(\alpha)} + p_{n-3,n-1,n}^{(\alpha)} + q_{n-3,n-1,n}^{(\alpha)}, & k = n-3, \\ p_{k,n-1,n}^{(\alpha)} + q_{k,n-1,n}^{(\alpha)}, & k = n-2, n-1. \end{cases}$$

When $n \geq 8$ and is even,

$$Q_{k,n}^{(\alpha)} = \begin{cases} p_{0,2,n}^{(\alpha)}, & k = 0, \\ p_{2m+1,2m+2,n}^{(\alpha)}, & k = 2m+1, m = 0, 1, \cdots, \frac{n-6}{2}, \\ p_{2m,2m,n}^{(\alpha)} + p_{2m,2m+2,n}^{(\alpha)}, & k = 2m, m = 1, \cdots, \frac{n-4}{2}, \\ p_{k,n-2,n}^{(\alpha)} + q_{k,n-1,n}^{(\alpha)}, & k = n-3, n-2, \\ q_{n-1,n-1,n}^{(\alpha)}, & k = n-1. \end{cases}$$

For implementation purposes, the coefficients $Q_{k,n}^{(\alpha)}$ for $k = n-3, n-2, n-1$ can be computed directly from the definitions of $p_{k,b,n}^{(\alpha)}$ and $q_{k,n-1,n}^{(\alpha)}$ using numerical quadrature since the integrands involve only explicitly known Lagrange basis functions and the kernel.

Therefore, a compact form of (2.4) is given by

$$\int_0^{t_n} (t_n - s)^{-\alpha} K(t_n, s)\, u(s)\, \mathrm{d}s \approx \sum_{k=0}^{n-1} Q_{k,n}^{(\alpha)} u(t_k), \quad 1 \leq n \leq N.$$

Although the above definitions distinguish between odd and even values of n, the construction of $Q_{k,n}^{(\alpha)}$ follows a unified principle: On each subinterval $[t_{2k}, t_{2k+2}]$, a quadratic interpolation is employed, and on the final subinterval, which may cover one or two steps depending on the parity of n, a quadratic interpolation over the last three nodes is used. Moreover, these coefficients satisfy certain boundedness properties, which will be established in Lemma 3.4.

By implementing the above approximation on Eq (1.1), we propose the numerical scheme as

$$t_n{}^{\beta} u_n = f(t_n) + \sum_{k=0}^{n-1} Q_{k,n}^{(\alpha)} u_k, \quad 1 \leq n \leq N, \tag{2.5}$$

where $Q_{k,n}^{(\alpha)}$ represents approximation coefficients defined above and u_k is the numerical solution of u at t_k. We call scheme (2.5) the fractional Adams-Simpson-type method.

3. Properties of the fractional Adams-Simpson-type method for VIE3

In this section, the local truncation error, convergence, and stability of the proposed scheme for VIE3 (1.1) are studied.

3.1. Local truncation error analysis

Subtracting scheme (2.5) from scheme (2.3) gives

$$t_n^{\beta} \cdot u(t_n) = f(t_n) + \sum_{k=0}^{n-1} Q_{k,n}^{(\alpha)} u(t_k) + R_n, \tag{3.1}$$

where R_n is the local truncation error given by

$$R_n = \int_0^{t_n} (t_n - s)^{-\alpha} K(t_n, s)\, u(s)\, \mathrm{d}s - \sum_{k=0}^{n-1} Q_{k,n}^{(\alpha)} u(t_k).$$

Combined with the definition of the interpolation error given in (2.2), we get

$$R_1 = \int_{t_0}^{t_1} (t_1 - s)^{-\alpha} K(t_1, s)\, R_{0,0} u(s)\, \mathrm{d}s, \quad R_2 = \int_{t_0}^{t_2} (t_2 - s)^{-\alpha} K(t_2, s)\, R_{1,1} u(s)\, \mathrm{d}s,$$

$$R_n = \begin{cases} \sum_{k=0}^{(n-3)/2} \int_{t_{2k}}^{t_{2k+2}} \frac{K(t_n, s) R_{2,2k+2} u(s)}{(t_n - s)^{\alpha}} \mathrm{d}s + \int_{t_{n-1}}^{t_n} \frac{K(t_n, s) R_{2,n-1} u(s)}{(t_n - s)^{\alpha}} \mathrm{d}s, n \geq 3 \text{ is odd}, \\ \sum_{k=0}^{(n-4)/2} \int_{t_{2k}}^{t_{2k+2}} \frac{K(t_n, s) R_{2,2k+2} u(s)}{(t_n - s)^{\alpha}} \mathrm{d}s + \int_{t_{n-2}}^{t_n} \frac{K(t_n, s) R_{2,n-1} u(s)}{(t_n - s)^{\alpha}} \mathrm{d}s, n \geq 4 \text{ is even}. \end{cases}$$

By construction, R_n consists of the interpolation error from replacing $u(s)$ by its piecewise Lagrange interpolant, integrated against the weakly singular kernel. The explicit decomposition of R_n in terms of the interpolation remainders $R_{a,b}u(s)$ is given in the following lemma.

Lemma 3.1. *Let Assumption 2.1 hold. For $t > 0$, it has [17]*

$$R_{0,0} u(t) = t \int_0^1 u'(st)\, \mathrm{d}s, \tag{3.2}$$

$$R_{1,1} u(t) = -\sum_{k=0}^{1} l_{k,1,1}(t)\, (t - t_k)^2 \int_0^1 u^{(2)}(t_k(1 - s) + ts)\, \mathrm{d}s, \tag{3.3}$$

$$R_{2,2} u(t) = -\sum_{k=0}^{2} l_{k,2,2}(t) (t - t_k)^2 \int_0^1 u^{(2)}(t_k(1 - s) + ts)\, s \mathrm{d}s, \tag{3.4}$$

$$R_{2,b} u(t) = \frac{1}{2} \sum_{k=b-2}^{b} l_{k,2,b}(t)\, (t - t_k)^3 \int_0^1 u^{(3)}(t_k(1 - s) + ts) s^2 \mathrm{d}s, \quad b \geq 2. \tag{3.5}$$

In addition, the function $K(t, s)$ mentioned in (1.1) is a continuous function, which is bounded in a finite closed interval. This is a property frequently utilized in the subsequent inequality estimates of the relevant terms. We now proceed to analyze the local truncation error.

Choose the non-uniform grid $0 = t_0 < t_1 < \cdots < t_N = T$ with $\tau_n = t_n - t_{n-1}$ incorporating a tunable parameter $\lambda \geq 1$, where λ-dependent coefficients ρ_1 and ρ_2 govern the non-uniform grid configuration through

(i) $\rho_1 \leq \dfrac{\tau_n}{\tau_{n+1}} \leq 1, \quad 1 \leq n \leq N - 1;$

(ii) $\tau_n = \rho_2 N^{-1} t_n^{1-\frac{1}{\lambda}}, \quad 1 \le n \le N;$

(iii) $\tau_{n+1} - \tau_n \le \rho_2 N^{-2} t_n^{1-\frac{2}{\lambda}}, \quad 2 \le n \le N-1;$

(iv) $t_n \le \rho_2 t_{n-1}, \quad 2 \le n \le N.$

Such grids have shown excellent performance in solving similar problems; see the literature [13, 18–21] for details. Note that $\sigma \in (0,1)$ and $\alpha \in [0,1)$ imply $\sigma + 1 - \alpha > 0$, then the error bound of the local truncation error in the following theorem decays as $N \to \infty$.

Theorem 3.1. *Assume that the solution u of VIE3 (1.1) satisfies Assumption 2.1, then the local truncation error R_n satisfies*

$$\begin{aligned} &|R_n| \le CN^{-\lambda(\sigma+1-\alpha)}, \quad n = 1, 2, \\ &|R_n| \le CN^{-\min\{\lambda(\sigma+1-\alpha), 4-\alpha\}}, \quad 3 \le n \le N. \end{aligned} \tag{3.6}$$

Proof. From (3.2) and (2.1), we have

$$\left|R_{0,0}u(t)\right| \le Ct \int_0^1 (st)^{\sigma-1} \mathrm{d}s = \frac{C}{\sigma} t^{\sigma}. \tag{3.7}$$

Thus, by using the conditions of non-uniform grid configuration (i), (ii) and scheme (3.7), and employing the beta function, we have

$$|R_1| \le \frac{C}{\sigma} \int_{t_0}^{t_1} (t_1 - s)^{-\alpha} |K(t_1, s)| s^{\sigma} \mathrm{d}s \le \frac{C}{\sigma} \int_{t_0}^{t_1} (t_1 - s)^{-\alpha} s^{\sigma} \mathrm{d}s.$$

Let $s = t_1 u$, then $\mathrm{d}s = t_1 \mathrm{d}u$ and

$$\int_{t_0}^{t_1} (t_1 - s)^{-\alpha} s^{\sigma} \mathrm{d}s = t_1^{1-\alpha+\sigma} \int_0^1 (1-u)^{-\alpha} u^{\sigma} \mathrm{d}u = t_1^{1-\alpha+\sigma} B(1-\alpha, \sigma+1),$$

where $B(\cdot,\cdot)$ is the Beta function defined by $B(x,y) = \int_0^1 u^{x-1}(1-u)^{y-1}\mathrm{d}u$. Using the relation $B(1-\alpha, \sigma+1) = \Gamma(1-\alpha)\Gamma(\sigma+1)/\Gamma(2+\sigma-\alpha)$, we obtain

$$|R_1| \le \frac{C}{\sigma} t_1^{1-\alpha+\sigma} \frac{\Gamma(1-\alpha)\Gamma(\sigma+1)}{\Gamma(2+\sigma-\alpha)} \le CN^{-\lambda(1-\alpha+\sigma)}.$$

Then, from (3.3), (2.1), and the conditions of non-uniform grid configuration (iii), (iv), for $t \in (t_0, t_2)$, we have

$$\begin{aligned} \left|R_{1,1}u(t)\right| &\le \frac{|t-t_1|\, t^2}{\tau_1} \int_0^1 \left|u^{(2)}(ts)\right| s\mathrm{d}s + \frac{|t-t_1|\, t^2}{\tau_1} \int_0^1 \left|u^{(2)}(t_1(1-s)+ts)\right| s\mathrm{d}s \\ &\le C\,|t-t_1|\, t \left[\int_0^1 \left|u^{(2)}(ts)\right| s\mathrm{d}s + \int_0^1 \left|u^{(2)}(t_1(1-s)+ts)\right| s\mathrm{d}s\right] \\ &\le C\,|t-t_1|\, t^{\sigma-1}. \end{aligned}$$

Using the above equation, we can get

$$|R_2| \leq C \int_{t_0}^{t_2} (t_2 - s)^{-\alpha} |K(t_2, s)| |s - t_1| s^{\sigma-1} \mathrm{d}s \leq C N^{-\lambda(1-\alpha+\sigma)}.$$

Consider the case where $n \geq 3$ and is odd. We divide R_n into three parts as

$$R_n = R1_n + R2_n + R3_n,$$

where

$$\begin{aligned}
R1_n &= \int_{t_0}^{t_2} (t_n - s)^{-\alpha} K(t_n, s) R_{2,2} u(s) \mathrm{d}s, \\
R2_n &= \sum_{k=1}^{\frac{n-3}{2}} \int_{t_{2k}}^{t_{2k+2}} (t_n - s)^{-\alpha} K(t_n, s) R_{2,2k+2} u(s) \mathrm{d}s, \\
R3_n &= \int_{t_{n-1}}^{t_n} (t_n - s)^{-\alpha} K(t_n, s) R_{2,n-1} u(s) \mathrm{d}s.
\end{aligned}$$

This decomposition separates the contributions with different forms of the interpolation remainder, as given in Lemma 3.1.

(i) Estimation of $R1_n$

By using (3.5) and (2.1), it follows that, for $t \in (t_0, t_2)$, there is

$$\begin{aligned}
\left|R_{2,2} u(t)\right| &\leq C \left[t^2 \int_0^1 \left|u^{(2)}(ts)\right| s \mathrm{d}s + t \sum_{k=1}^{2} |t - t_k| \int_0^1 u^{(2)}(t_k(1-s) + ts) s \mathrm{d}s \right] \\
&\leq C t_2 t^{\sigma-1},
\end{aligned}$$

and thus we have

$$|R1_n| \leq C t_2 \int_{t_0}^{t_2} (t_n - s)^{-\alpha} K(t_n, s) s^{\sigma-1} \mathrm{d}s \leq C {t_2}^{\sigma+1-\alpha} \leq C N^{-\lambda(\sigma+1-\alpha)}.$$

(ii) Estimation of $R2_n$

From (3.5), for $k \geq 1$, we have

$$\begin{aligned}
R_{2,2k+2} u(t) &= \frac{1}{2} \sum_{m=2k}^{2k+2} l_{m,2,2k+2}(t) (t - t_m)^3 \int_0^1 u^{(3)}(t_m(1-s) + ts) s^2 \mathrm{d}s \\
&= \frac{1}{6} u^{(3)}(t_{2k+2}) \sum_{m=2k}^{2k+2} l_{m,2,2k+2}(t) (t - t_m)^3 + \frac{1}{2} \sum_{m=2k}^{2k+2} l_{m,2,2k+2}(t) (t - t_m)^3 u_{m,2k+1}(t),
\end{aligned}$$

where

$$u_{m,2k+1}(t) = \int_0^1 \left[u^{(3)}(t_m(1-s) + ts) - u^{(3)}(t_{2k+2}) \right] s^2 \mathrm{d}s.$$

Define $\omega_{2k}(t) = (t - t_{2k})(t - t_{2k+1})(t - t_{2k+2})$. According to divided difference theory, it holds that

$$\sum_{m=2k}^{2k+2} l_{m,2,2k+2}(t) (t - t_m)^3 = \omega_{2k}(t) \sum_{m=2k}^{2k+2} \frac{(t - t_m)^2}{\omega'_{2k}(t_m)} = \omega_{2k}(t).$$

Thus, it gets

$$R_{2,2k+2}u\left(t\right)=\frac{1}{6}u^{(3)}\left(t_{2k+2}\right)\omega_{2k}\left(t\right)+\frac{1}{2}\sum_{m=2k}^{2k+2}l_{m,2,2k+2}\left(t\right)(t-t_m)^3u_{m,2k+1}\left(t\right).$$

Based on the above equation, we rewrite that

$$R2_n=R21_n+R22_n,$$

where

$$R21_n=\frac{1}{6}\sum_{k=1}^{\frac{n-3}{2}}u^{(3)}\left(t_{2k+2}\right)\int_{t_{2k}}^{t_{2k+2}}(t_n-s)^{-\alpha}K\left(t_n,s\right)\omega_{2k}\left(s\right)\mathrm{d}s,$$

$$R22_n=\frac{1}{2}\sum_{k=1}^{\frac{n-3}{2}}\int_{t_{2k}}^{t_{2k+2}}(t_n-s)^{-\alpha}K\left(t_n,s\right)\sum_{m=2k}^{2k+2}l_{m,2,2k+2}\left(s\right)(s-t_m)^3u_{m,2k+1}\left(s\right)\mathrm{d}s.$$

Note that for odd n, the subintervals $[t_{2k}, t_{2k+2}]$ for $k=1,\ldots,(n-3)/2$ exactly cover the region $[t_2, t_{n-1}]$, matching the mesh index range.

Next, we first estimate $R21_n$, so we define

$$\bar{\omega}_{2k}^{*}\left(t\right)=\int_{t}^{t_{2k+2}}\omega_{2k}\left(s\right)\mathrm{d}s.$$

Then, using the integration by parts, we get

$$\begin{aligned}R21_n=&\tfrac{1}{6}\sum_{k=1}^{\frac{n-3}{2}}u^{(3)}\left(t_{2k+2}\right)\left(t_n-t_{2k}\right)^{-\alpha}K\left(t_n,t_{2k}\right)\overline{\omega}_{2k}^{*}\left(t_{2k}\right)\\&+\tfrac{1}{6}\sum_{k=1}^{\frac{n-3}{2}}u^{(3)}\left(t_{2k+2}\right)\int_{t_{2k}}^{t_{2k+2}}\left[\alpha(t_n-s)^{-\alpha-1}K\left(t_n,s\right)+(t_n-s)^{-\alpha}\tfrac{\partial K(t_n,s)}{\partial s}\right]\overline{\omega}_{2k}^{*}\left(s\right)\mathrm{d}s.\end{aligned}$$

The first and second items in the above formula are recorded as

$$R21_{1,n}=\frac{1}{6}\sum_{k=1}^{\frac{n-3}{2}}u^{(3)}\left(t_{2k+2}\right)\left(t_n-t_{2k}\right)^{-\alpha}K\left(t_n,t_{2k}\right)\overline{\omega}_{2k}^{*}\left(t_{2k}\right),$$

$$R21_{2,n}=\frac{1}{6}\sum_{k=1}^{\frac{n-3}{2}}u^{(3)}\left(t_{2k+2}\right)\int_{t_{2k}}^{t_{2k+2}}\left[\alpha(t_n-s)^{-\alpha-1}K\left(t_n,s\right)+(t_n-s)^{-\alpha}\frac{\partial K\left(t_n,s\right)}{\partial s}\right]\overline{\omega}_{2k}^{*}\left(s\right)\mathrm{d}s,$$

and

$$\begin{aligned}\left|R21_{1,n}\right|\leq C&\max_{1\leq k\leq\frac{n-3}{2}}\left\{t_{2k+2}^{\sigma+1-\alpha-3}(\tau_{2k+2}+\tau_{2k+1})^2\left(\tau_{2k+2}-\tau_{2k+1}\right)\right\}\\&\times\sum_{k=1}^{\frac{n-3}{2}}\left(t_n-t_{2k}\right)^{-\alpha}\left|K\left(t_n,t_{2k}\right)\right|t_{2k+2}^{\alpha-1}\left(t_{2k+2}-t_{2k}\right).\end{aligned}$$

Through simple calculation, we establish that

$$\sum_{k=1}^{\frac{n-3}{2}}(t_n - t_{2k})^{-\alpha}\left|K(t_n, t_{2k})\right| t_{2k+2}^{\alpha-1}(t_{2k+2} - t_{2k}) \le C\sum_{k=1}^{\frac{n-3}{2}}\int_{t_{2k}}^{t_{2k+2}}(t_n - s)^{-\alpha}s^{\alpha-1}\,\mathrm{d}s$$
$$\le C\int_{t_0}^{t_n}(t_n - s)^{-\alpha}s^{\alpha-1}\,\mathrm{d}s = C\mathrm{B}(\alpha, 1-\alpha).$$

We get

$$\left|R21_{1,n}\right| \le C\max_{1\le k\le\frac{n-3}{2}}\left\{t_{2k+2}^{\sigma+1-\alpha-3}(\tau_{2k+2} + \tau_{2k+1})^2(\tau_{2k+2} - \tau_{2k+1})\right\}.$$

Define $\gamma = \min\left\{\frac{\lambda}{2}(\sigma + 1 - \alpha), 2\right\}$. It holds that

$$\left|R21_{1,n}\right| \le C\max_{1\le k\le\frac{n-3}{2}}\left\{t_{2k+2}^{\sigma+1-\alpha}\left(\frac{\tau_{2k+2}}{t_{2k+2}}\right)^2\left(\frac{\tau_{2k+2} - \tau_{2k+1}}{t_{2k+2}}\right)\right\}$$
$$\le C\max_{1\le k\le\frac{n-3}{2}}\left\{t_{2k+2}^{\sigma+1-\alpha}\left(\frac{\tau_{2k+2}}{t_{2k+2}}\right)^{\gamma}\left(\frac{\tau_{2k+2} - \tau_{2k+1}}{t_{2k+2}}\right)^{\frac{\gamma}{2}}\right\}$$
$$\le CN^{-2\gamma}\max_{1\le k\le\frac{n-3}{2}}\left\{t_{2k+2}^{\sigma+1-\alpha-\frac{2\gamma}{\lambda}}\right\} \le CN^{-2\gamma} = CN^{-\min\{\lambda(\sigma+1-\alpha),4\}}.$$

Consider $R21_{2,n}$. We have

$$|R21_{2,n}| \le C\sum_{k=1}^{(n-3)/2}t_{2k+2}^{\sigma-3}\int_{t_{2k}}^{t_{2k+2}}\left|\alpha(t_n - s)^{-\alpha-1}K(t_n, s) + (t_n - s)^{-\alpha}\frac{\partial K(t_n, s)}{\partial s}\right||\overline{\omega}_{2k}^{*}(s)|\,\mathrm{d}s.$$

Reuse the conditions of the non-uniform grid configuration. We get

$$\left|R21_{2,n}\right| \le C\max_{1\le k\le\frac{n-3}{2}}\left\{t_{2k+2}^{\sigma-3}\tau_{2k+2}^{4}\right\}\tau_n^{-\alpha}$$
$$= C\max_{1\le k\le\frac{n-3}{2}}\left\{t_{2k+2}^{\sigma+1-\alpha}\left(\frac{\tau_{2k+2}}{t_{2k+2}}\right)^{3+1-\alpha}\tau_{2k+2}^{\alpha}\right\}\tau_n^{-\alpha}$$
$$\le C\max_{1\le k\le\frac{n-3}{2}}\left\{t_{2k+2}^{\sigma+1-\alpha}\left(\frac{\tau_{2k+2}}{t_{2k+2}}\right)^{\min\{\lambda(\sigma+1-\alpha),3+1-\alpha\}}\right\}$$
$$\le CN^{-\min\{\lambda(\sigma+1-\alpha),4-\alpha\}}\max_{1\le k\le\frac{n-3}{2}}\left\{t_{2k+2}^{\sigma+1-\alpha-\min\left\{\sigma+1-\alpha,\frac{4-\alpha}{\lambda}\right\}}\right\}$$
$$\le CN^{-\min\{\lambda(\sigma+1-\alpha),4-\alpha\}}.$$

So far, we know that

$$|R21_n| \le CN^{-\min\{\lambda(\sigma+1-\alpha),4-\alpha\}}.$$

Then, we continue to estimate $R22_n$. For $t \in (t_{2k}, t_{2k+2})$ and $m = 2k, 2k+1, 2k+2 (k \ge 1)$, it holds that

$$\left|u_{m,2k+1}(t)\right| \le \int_0^1\left|u^{(4)}(\xi_t)\right|\left|t_m(1-s) + ts - t_{2k+2}\right|s^2\mathrm{d}s$$
$$\le \frac{2}{3}(\tau_{2k+1} + \tau_{2k+2})\sup_{\eta\in(t_{2k},t_{2k+2})}\left|u^{(4)}(\eta)\right|,$$

and

$$\left|\sum_{m=2k}^{2k+2} l_{m,2,2k+2}(t)(t-t_m)^3\right| \le \frac{(\tau_{2k+1}+\tau_{2k+2})^4}{\tau_{2k+1}} + \frac{(\tau_{2k+1}+\tau_{2k+2})^5}{\tau_{2k+1}\tau_{2k+2}} + \frac{(\tau_{2k+1}+\tau_{2k+2})^4}{\tau_{2k+2}}.$$

Reusing (2.1) and the conditions of non-uniform grid configuration, we get

$$\begin{aligned}
|R22_n| &\le C \max_{1\le k\le \frac{n-3}{2}} \left\{\tau_{2k+2}^4 t_{2k+2}^{1-\alpha} t_{2k}^{\sigma-4}\right\} \int_{t_2}^{t_{n-1}} (t_n-s)^{-\alpha} s^{\alpha-1} ds \\
&\le C \max_{1\le k\le \frac{n-3}{2}} \left\{\left(\frac{\tau_{2k+2}}{t_{2k+2}}\right)^4 t_{2k+2}^{\sigma+1-\alpha}\right\} \le C \max_{1\le k\le \frac{n-3}{2}} \left\{\left(\frac{\tau_{2k+2}}{t_{2k+2}}\right)^{\min\{\lambda(\sigma+1-\alpha),4\}} t_{2k+2}^{\sigma+1-\alpha}\right\} \\
&\le CN^{-\min\{\lambda(\sigma+1-\alpha),4\}} \max_{1\le k\le \frac{n-3}{2}} \left\{t_{2k+2}^{\sigma+1-\alpha-\min\left\{\sigma+\alpha,\frac{4}{\lambda}\right\}}\right\} \le CN^{-\min\{\lambda(\sigma+1-\alpha),4\}}.
\end{aligned}$$

Therefore, we can conclude that

$$|R2_n| \le CN^{-\min\{\lambda(\sigma+1-\alpha),4-\alpha\}}.$$

(iii) Estimation of $R3_n$

For the purpose of estimating $R3_n$, we begin by giving a bound of $R_{2,n-1}u(t)$. When t belongs to (t_{n-1}, t_n), applying (2.1) leads to

$$\left|R_{2,n-1}u(t)\right| \le C\tau_n^3 t^{\sigma-3}. \tag{3.8}$$

Using (3.8), we can get

$$\begin{aligned}
|R3_n| &\le C\tau_n^3 \int_{t_{n-1}}^{t_n} (t_n-s)^{-\alpha} s^{\sigma-3} \mathrm{d}s \\
&\le C t_{n-1}^{\sigma-3} \tau_n^{3+1-\alpha} \le C t_{n-1}^{\sigma+1-\alpha} \left(\frac{\tau_{n-1}}{t_{n-1}}\right)^{\min\{\lambda(\sigma+1-\alpha),3+1-\alpha\}} \\
&\le CN^{-\min\{\lambda(\sigma+1-\alpha),4-\alpha\}}.
\end{aligned}$$

In summary, conclusion (3.6) holds for all $n \ge 3$, and n is odd. The proof for even n follows a similar argument to the odd case and is thus omitted for brevity.

3.2. Convergence analysis

We first give the fractional Grönwall inequalities that are needed in the following proof.

Lemma 3.2 (A fractional Grönwall inequality [22])**.** *Let g_0 and C_0 be two positive constants, the step length be $\tau_{j+1} = t_{j+1} - t_j$, and $\{\varphi_n\}_0^N$ be a set function that satisfy*

$$\varphi_0 \le g_0, \quad \varphi_k \le C_0 \sum_{j=0}^{k-1} \tau_{j+1} \left(t_k - t_j\right)^{-\alpha} \varphi_j + g_0$$

for $k = 1, 2, \cdots, N$. Then, it holds that

$$\varphi_n \le \varepsilon(1-\alpha) g_0,$$

where

$$\varepsilon(1-\alpha) = E_{1-\alpha}\left(C_0\Gamma(1-\alpha)\,T^{1-\alpha}\right), \tag{3.9}$$

with C_0 being the same constant as in the assumption above. For $\mu = 1-\alpha \in (0,1]$, the Mittag-Leffler functions $E_\mu(z)$ are defined as

$$E_\mu(z) = \sum_{k=0}^{\infty} \frac{z^k}{\Gamma(k\mu+1)}, \tag{3.10}$$

which converge for all $z \in \mathbb{C}$.

Lemma 3.3 (A modified fractional Grönwall inequality [17])**.** *Let g_0, C_0, and δ be positive constants and $\{\mathrm{X}_n\}_0^N$ be a set function that satisfy*

(i) For any $1 \le n \le N$, if $\max\limits_{0\le k\le n-1} \mathrm{X}_k \le \delta$, then $\mathrm{X}_n \le C_0 \sum\limits_{k=0}^{n-1} \tau_{k+1}(t_n - t_k)^{-\alpha}\mathrm{X}_k + g_0$.

(ii) $\mathrm{X}_0 \le g_0$, $\varepsilon(1-\alpha)\,g_0 \le \delta$, where $\varepsilon(1-\alpha)$ is defined by (3.9).

Then, for all $0 \le n \le N$, we have $\mathrm{X}_n \le \varepsilon(1-\alpha)\,g_0$.

The threshold δ takes different values depending on the specific problem.

Lemma 3.4. *Assume that the non-uniform grid configuration assumption (i) holds, then the coefficients $Q_{k,n}^{\alpha}$ satisfy*

$$\left|Q_{k,n}^{(\alpha)}\right| \le C\tau_{k+1}(t_n - t_k)^{-\alpha}, \quad 0 \le k \le n-1, \quad 1 \le n \le N. \tag{3.11}$$

Proof. Obviously, there is

$$\begin{aligned}
\left|q_{0,0,1}^{(\alpha)}\right| &= \left|\int_{t_0}^{t_1} (t_1 - s)^{-\alpha} K(t_1, s)\,\mathrm{d}s\right| \le C\int_{t_0}^{t_1} (t_1 - s)^{-\alpha}\,\mathrm{d}s = C\frac{\tau_1^{-\alpha+1}}{-\alpha+1} \le C\tau_1(t_1 - t_0)^{-\alpha},\\
\left|q_{k,1,2}^{(\alpha)}\right| &= \left|\int_{t_0}^{t_2} (t_2 - s)^{-\alpha} K(t_2, s)\, l_{k,1,1}(s)\,\mathrm{d}s\right| \le C\int_{t_0}^{t_2} (t_2 - s)^{-\alpha}\,\mathrm{d}s \le C(t_2 - t_0)^{-\alpha+1}\\
&= Ct_2(t_2 - t_0)^{-\alpha} \le C\tau_{k+1}(t_2 - t_k)^{-\alpha}, \quad k = 0, 1.
\end{aligned}$$

When $n \ge 3$ and $k = n-3, n-2, n-1$, we have

$$\left|q_{k,n-1,n}^{(\alpha)}\right| \le \begin{cases} C\int_{t_{n-1}}^{t_n} (t_n - s)^{-\alpha}\mathrm{d}s \le C\tau_{k+1}(t_n - t_k)^{-\alpha}, & n \text{ is odd},\\ C\int_{t_{n-2}}^{t_n} (t_n - s)^{-\alpha}\mathrm{d}s \le C\tau_{k+1}(t_n - t_k)^{-\alpha}, & n \text{ is even}. \end{cases}$$

Next, we will estimate $p_{k,b,n}^{(\alpha)}$ for $n \ge 3$, $2 \le b \le n-1$, $k = b-2, b-1, b$. By the definition of $p_{k,b,n}^{(\alpha)}$ and (i), we have

$$\begin{aligned}
\left|p_{k,b,n}^{(\alpha)}\right| &= \left|\int_{t_{b-2}}^{t_b} (t_n - s)^{-\alpha} K(t_n, s)\, l_{k,2,b}(s)\mathrm{d}s\right| \le C\int_{t_{b-2}}^{t_b} (t_n - s)^{-\alpha}\mathrm{d}s\\
&\le C(\tau_b + \tau_{b+1})(t_n - t_b)^{-\alpha} \le C\tau_{k+1}(t_n - t_b)^{-\alpha}.
\end{aligned}$$

Since $0 < \alpha < 1$, we have

$$\begin{aligned}(t_n - t_b)^{-\alpha} &= (t_n - t_k)^{-\alpha}\left(\frac{t_n - t_b}{t_n - t_k}\right)^{-\alpha} \le (t_n - t_k)^{-\alpha}\left(\frac{t_n - t_b}{t_n - t_{b-2}}\right)^{-\alpha} \\ &\le (t_n - t_k)^{-\alpha}\left(\frac{t_{b+1} - t_b}{t_{b+1} - t_{b-2}}\right)^{-\alpha} = (t_n - t_k)^{-\alpha}\left(\frac{\tau_b}{\tau_{b-1} + \tau_b + \tau_{b+1}}\right)^{-\alpha} \\ &\le 3^{-\alpha}(t_n - t_k)^{-\alpha}.\end{aligned}$$

This leads to

$$\left|p_{k,b,n}^{(\alpha)}\right| \le C\tau_{k+1}(t_n - t_k)^{-\alpha}, \quad n \ge 3, \quad 2 \le b \le n-1, \quad k = b-2, b-1, b.$$

By the definition of the coefficient $Q_{k,n}^{(\alpha)}$ and combining the above equations, we can get that (3.11) holds.

Now, we are at the position of the following theorem.

Theorem 3.2. *Let the solution $u(t)$ of VIE3 (1.1) satisfy Assumption 2.1 and u_n be the numerical solution of the fractional Adams-Simpson-type scheme (2.5) with the grid satisfying the assumptions (i)–(iv). Then, there exists a constant $N_0 > 0$, independent of N and n, such that for all $N \ge N_0$, it holds that*

$$|u(t_n) - u_n| \le CN^{\lambda\beta - \min\{\lambda(\sigma+1-\alpha),4-\alpha\}}, \quad 0 \le n \le N. \tag{3.12}$$

Proof. Let $e_n = u(t_n) - u_n$. From (2.5) and (3.1), we have

$$e_0 = 0, \quad e_n = t_n^{-\beta}\left(\sum_{k=0}^{n-1} Q_{k,n}^{(\alpha)}\left[u(t_k) - u_k\right] + R_n\right), \quad 1 \le n \le N.$$

Taking the absolute value and applying Theorem 3.1 and Lemma 3.4, we have

$$|e_n| \le Ct_n^{-\beta}\left[\sum_{k=0}^{n-1} \tau_{k+1}(t_n - t_k)^{-\alpha}|e_k| + N^{-\min\{\lambda(\sigma+1-\alpha),4-\alpha\}}\right].$$

Then, from the grid assumptions (ii) and (iv), noting that $t_n = (n/N)^\lambda T \ge N^{-\lambda}T$, it follows that

$$t_n^{-\beta} \le T^{-\beta}N^{\lambda\beta}. \tag{3.13}$$

Therefore,

$$|e_n| \le C_0 \sum_{k=0}^{n-1} \tau_{k+1}(t_n - t_k)^{-\alpha}|e_k| + g_0,$$

where $C_0 = T^{-\beta}N^{\lambda\beta}$, $g_0 = CN^{\lambda\beta - \min\{\lambda(\sigma+1-\alpha),4-\alpha\}}$. Let $N \ge N_0$ be a sufficiently large number. From the definition (3.9), we have

$$\varepsilon(1-\alpha)g_0 = C\varepsilon(1-\alpha)N^{\lambda\beta - \min\{\lambda(\sigma+1-\alpha),4-\alpha\}} \le 1.$$

Therefore, the nonnegative set function $\{|e_n|\}_0^N$ satisfies the conditions of Lemma 3.3 when $N \ge N_0$. Thus, it can be obtained that

$$|e_n| \le \varepsilon(1-\alpha)g_0 = C\varepsilon(1-\alpha)N^{\lambda\beta - \min\{\lambda(\sigma+1-\alpha),4-\alpha\}}.$$

This shows that (3.12) holds.

Theorem 3.2 rigorously validates that the fractional Adams-Simpson-type scheme (2.5) with the non-uniform grid guarantees a minimum convergence rate of $\min\{\lambda(\sigma+1-\alpha), 4-\alpha\} - \lambda\beta$ for the VIE3, which fulfills Assumption 2.1. The optimal convergence order is achieved when the two terms inside the minimum are balanced, i.e., $\lambda(\sigma+1-\alpha) = 4-\alpha$, which gives the optimal grid parameter $\lambda = (4-\alpha)/(\sigma+1-\alpha)$. The resulting convergence order is $4-\alpha-\lambda\beta$. Excessive λ values induce nodal clustering proximal to $t = 0$; when $\lambda \geq (4-\alpha)/(\sigma+1-\alpha)$, the convergence order decreases with increasing λ. Otherwise, if $\lambda \leq (4-\alpha)/(\sigma+1-\alpha)$, the convergence order increases with the increase of λ. Therefore, $\lambda = (4-\alpha)/(\sigma+1-\alpha)$ is recommended as the optimal choice of grid parameter. For instance, when $\sigma \approx 0.5$ and $\alpha = 0.1$, the optimal grading parameter is $\lambda \approx 2.79$. If λ is chosen smaller than this optimal value, the term $\lambda(\sigma+1-\alpha)$ dominates the error; otherwise, the term $4-\alpha$ dominates. Moreover, note that the exponent in (3.12) may become negative if β is sufficiently large. In such cases, the convergence order can be improved by choosing a smaller λ, though the optimal theoretical rate is limited by the singularity strength. This reflects an inherent feature of VIE3 with a strongly degenerate factor t^{β}.

3.3. Stability analysis

This section conducts a sensitivity analysis of the numerical solution u_n under initial value disturbances. Consider perturbations of the form $u_0 \to u_0 + \phi_0$ in the governing Eq (2.5), where ϕ_0 represents bounded variations. Let $\tilde{u}_n$ denote the resulting perturbed solution generated by the modified initial condition.

Theorem 3.3. *Let the approximation u_n be constructed using the scheme (2.5) with the grid assumptions (i)–(iv). Then, for a sufficiently small $u_0 + \phi_0$, it holds that*

$$|u_n - \tilde{u}_n| \leq C|\phi_0|, \quad 0 \leq n \leq N. \tag{3.14}$$

Proof. Let $\tilde{z}_n = \tilde{u}_n - u_n$. We have the following perturbation scheme:

$$\begin{cases} \tilde{z}_n = t_n^{-\beta} \sum\limits_{k=0}^{n-1} Q_{k,n}^{(\alpha)} (\tilde{u}_k - u_k), 1 \leq n \leq N, \\ \tilde{z}_0 = \phi_0. \end{cases}$$

Taking absolute values and employing (3.13) leads to

$$|\tilde{z}_n| \leq CN^{\lambda\beta} \sum_{k=0}^{n-1} \left|Q_{k,n}^{(\alpha)}\right| |\tilde{u}_k - u_k|.$$

Using Lemma 3.4 it can be obtained that

$$|\tilde{z}_n| \leq C_0 \sum_{k=0}^{n-1} \tau_{k+1} (t_n - t_k)^{-\alpha} |\tilde{z}_k| + g_0,$$

where $C_0 = CN^{\lambda\beta}$, $g_0 = |\phi_0|$. When $|\varphi_0|$ is sufficiently small, $\varepsilon(1-\alpha) g_0 = \varepsilon(1-\alpha)|\phi_0| \leq 1/2$. Finally, using Lemma 3.3, we can obtain $|\tilde{z}_n| \leq \varepsilon(1-\alpha) g_0 = \varepsilon(1-\alpha)|\phi_0|$, which completes the proof.

The constant C in (3.14) may depend on N and the problem parameters through the Mittag-Leffler function.

3.4. Computational complexity

We briefly discuss the computational cost of the proposed scheme (2.5). At each time step t_n, the numerical solution u_n is obtained via an explicit recurrence, which requires $O(n)$ operations. Summing over all $n = 1, \ldots, N$, the total cost of the time-stepping procedure is $O(N^2)$. The coefficients $Q_{k,n}^{(\alpha)}$ are computed by numerical quadrature over the corresponding subintervals, with each coefficient requiring $O(1)$ operations. Since there are $O(N^2)$ coefficients in total, the precomputation also requires $O(N^2)$ operations, and the storage requirement is $O(N^2)$ to store the coefficient matrix.

For a given accuracy tolerance, the non-uniform graded mesh requires significantly fewer nodes than a uniform mesh to resolve the initial singularity. Within the block discrete framework, the piecewise quadratic interpolation further allows the coefficients to be evaluated efficiently by organizing the integrals over shared subintervals. Consequently, although the asymptotic complexity with respect to N is $O(N^2)$, the actual computational effort to achieve a prescribed accuracy is substantially reduced compared with uniform-mesh methods.

4. Numerical experiments

In this section, the effectiveness of the fractional Adams-Simpson-type algorithm is verified by several numerical experiments. In these examples, a non-uniform grid with parameter $\lambda \geq 1$ is used, and its nodes are constructed as $t_n = (n/N)^{\lambda} T$, $0 \leq n \leq N$, where N represents the number of total subdivision steps. To evaluate the precision of the numerical solution, each example selects a test problem with an analytical solution for comparative analysis by calculating the maximum absolute error $E(N) = \max\limits_{0 \leq n \leq N} |u(t_n) - u_n|$ between the numerical solution and the exact solution in $T = 1$ and analyzing the convergence order $O(N) = \log_2 [E(N)/E(2N)]$.

Example 1. *Consider the VIE3* (1.1) *in the case* $\beta = 1$ *defined in the interval* $t \in [0, 1]$ *with* $K(t, s) = 1/2$ *and*

$$f(t) = t^{\frac{7}{2}} - \frac{1}{2} \int_0^t (t - s)^{-\alpha} s^{\frac{5}{2}} \mathrm{d}s.$$

The exact solution of (1.1) *is* $u(t) = t^{5/2}$. *We solve the problem using the numerical scheme (2.5) with different values of* α *and* λ. *The results are presented in Table 1. It shows that the fractional Adams-Simpson-type algorithm achieves its theoretical convergence order of* $4 - \alpha - \lambda\beta$ *when* $\lambda = 2.5$ *for the case* $\beta = 1$. *Moreover, the convergence order decreases as* λ *increases with other parameters fixed, which aligns with the theoretical analysis in Theorem 3.2.*

To assess the performance of the proposed fractional Adams-Simpson-type method, we compare it with the standard fractional Euler method on a uniform mesh, which approximates the integral in (1.1) *using the left rectangular rule [23].*

Table 2 compares the errors and convergence orders of the fractional Euler method on a uniform mesh and the proposed method on a graded mesh with $\lambda = 2.5$ *and* $\lambda = 2$. *It can be observed that the proposed method achieves substantially higher accuracy and faster convergence than the Euler method. The convergence order of the Euler method remains around* 0.95, *whereas the proposed method achieves orders around* 2. *These results clearly demonstrate the superior accuracy and efficiency of the proposed fractional Adams-Simpson-type method.*

Table 1. Maximum errors and convergence orders for the fractional Adams-Simpson-type scheme (2.5) applied to Example 1 with $\beta = 1$.

λ	N	$\alpha = 0.1$		$\alpha = 0.15$		$\alpha = 0.2$	
		E(N)	O(N)	E(N)	O(N)	E(N)	O(N)
2.5	2^4	1.9256e-02	1.11	2.0114e-02	1.05	2.1036e-02	1.05
	2^5	8.9121e-03	1.63	9.4896e-03	1.64	1.0128e-02	1.65
	2^6	2.8870e-03	1.97	3.0527e-03	2.10	3.2259e-03	2.28
	2^7	7.3556e-04	–	7.1278e-04	–	6.6473e-04	–
3	2^4	2.0011e-02	0.89	2.0750e-02	0.86	2.1530e-02	0.82
	2^5	1.0792e-02	1.51	1.1444e-02	1.51	1.2161e-02	1.51
	2^6	3.7897e-03	1.88	4.0199e-03	1.97	4.2657e-03	2.09
	2^7	1.0285e-03	–	1.0276e-03	–	1.0012e-03	–
3.5	2^4	1.9805e-02	0.67	2.0378e-02	0.63	2.0962e-02	0.59
	2^5	1.2465e-02	1.40	1.3165e-02	1.39	1.3933e-02	1.38
	2^6	4.7301e-03	1.80	5.0235e-03	1.86	5.3395e-03	2.07
	2^7	1.3556e-03	–	1.3802e-03	–	2.7080e-02	–

Table 2. Comparison of the fractional Euler method on a uniform mesh and the proposed fractional Adams-Simpson-type method on a graded mesh for Example 1 with $\beta = 1$.

α	N	Fractional Euler method		Proposed method $\lambda = 2.5$		Proposed method $\lambda = 2$	
		E(N)	O(N)	E(N)	O(N)	E(N)	O(N)
0.05	2^4	2.0854e-02	0.93	1.8446e-02	1.14	1.9239e-02	0.70
	2^5	1.0694e-02	0.96	8.3794e-03	1.62	1.1814e-02	1.41
	2^6	5.4146e-03	0.98	2.7258e-03	1.88	1.3171e-03	2.00
	2^7	2.7241e-03	0.99	7.3899e-04	2.12	3.2919e-04	2.34
	2^8	1.3662e-03	0.99	1.6967e-04	–	6.4932e-05	–

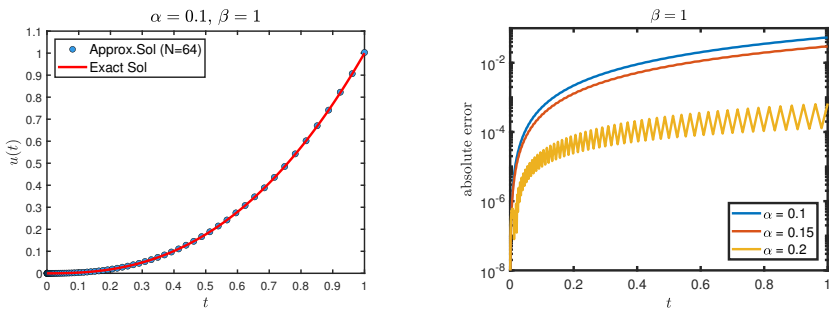

(a) (b)

Figure 1. Graphs of $u(t)$ and the absolute error for Example 1 with $\beta = 1$. (a) Comparison of the exact solution (red curve) and numerical approximations (blue markers) for $\lambda = 2.5$. (b) Absolute error at each node for different values of α and $\lambda = 2.5$.

The graphs of $u(t)$ and the absolute error $E(N)$ are shown in Figure 1. Figure 1 intuitively shows the accuracy of the numerical method for VIE3 (1.1) *with $\beta = 1$.*

Example 2. *Consider the VIE3* (1.1) *in the case $\beta = 1.5$ on the interval $t \in [0, 1]$ with parameters $K(t, s) = \frac{1}{\sqrt{2\pi}} s$ and*

$$f(t) = t^{\frac{33}{10}} - \frac{1}{\sqrt{2\pi}} \int_0^t (t-s)^{-\alpha} s^{\frac{14}{5}} \mathrm{d}s.$$

The exact solution of (1.1) *in this case is $u(t) = t^{\frac{9}{5}}$. We apply the numerical scheme (2.5) for different values of α and λ, and the results are summarized in Table 3.*

From Table 3, the theoretical convergence order $4 - \alpha - \lambda\beta$ is achieved when $\lambda = 2.5$ for VIE3 (1.1) *in the case $\beta > 1$. For fixed α and β, the convergence order decreases as λ increases, consistent with Theorem 3.2.*

Table 3. Maximum errors and convergence orders for the fractional Adams-Simpson-type scheme (2.5) applied to Example 2 with $\beta = 1.5$.

λ	N	$\alpha = 0.1$		$\alpha = 0.2$		$\alpha = 0.25$	
		E(N)	O(N)	E(N)	O(N)	E(N)	O(N)
2.5	2^4	3.6034e-03	1.14	3.8385e-03	1.18	3.9583e-03	1.20
	2^5	1.6317e-03	1.74	1.6976e-03	2.05	1.7208e-03	2.31
	2^6	4.8691e-04	2.43	4.1051e-04	4.09	3.4810e-04	1.64
	2^7	9.0386e-05	–	2.4041e-05	–	1.1185e-04	–
3	2^4	3.7028e-03	0.93	3.9328e-03	0.95	4.0519e-03	0.97
	2^5	1.9380e-03	1.61	2.0323e-03	1.82	2.0725e-03	1.99
	2^6	6.3613e-04	2.24	5.7462e-04	4.11	5.2206e-04	2.88
	2^7	1.3483e-04	–	3.3296e-05	–	7.0962e-05	–
4	2^4	3.5769e-03	0.55	4.0392e-03	0.58	3.9115e-03	0.57
	2^5	2.4366e-03	1.36	2.7013e-03	1.67	2.6381e-03	1.57
	2^6	9.4751e-04	1.98	8.4651e-04	3.61	8.9061e-04	4.14
	2^7	2.4075e-04	–	2.7080e-02	–	5.0452e-05	–

Figure 2 shows the graphs of $u(t)$ and the absolute errors. The numerical results in Table 3 and Figure 2 confirm this theoretical prediction and the accuracy of the numerical method for VIE3 (1.1) *in the case $\beta > 1$.*

For this example, the comparison between the proposed method and the fractional Euler method yields similar conclusions to those in Example 1. The corresponding results are therefore omitted for brevity.

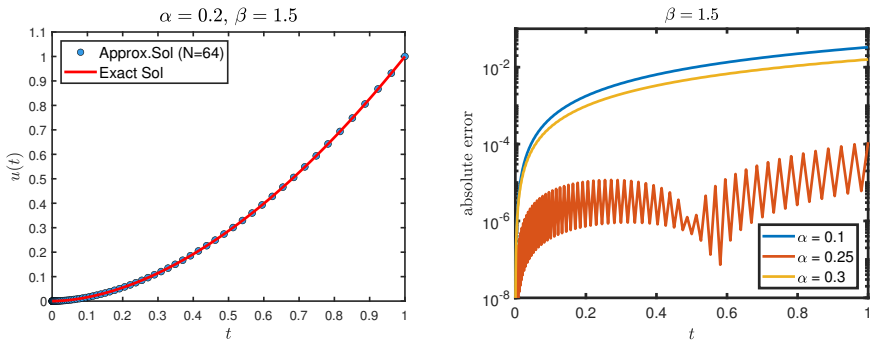

(a) (b)

Figure 2. Graphs of $u(t)$ and the absolute error for Example 2 with $\beta = 1.5$. (a) The contrast of the exact solution (red curve) against discrete numerical approximations (blue markers) with $\lambda = 2.5$. (b) The absolute error at each node under different α values and $\lambda = 2.5$.

Example 3. *Consider the VIE3* (1.1) *in the case* $\beta = 0.6$ *on the interval* $t \in [0, 1]$ *with parameters* $K(t, s) = 1$ *and*

$$f(t) = t^{\frac{34}{15}} - \int_0^t (t-s)^{-\alpha} s^{\frac{5}{3}} \mathrm{d}s.$$

The exact solution is $u(t) = t^{\frac{5}{3}}$. *We solve the problem using the numerical scheme (2.5) to vary* α *and* λ, *and the results are presented in Table 4.*

Consistent with the previous examples, the scheme achieves the theoretical convergence order $4 - \alpha - \lambda\beta$ *when* $\lambda = 2.5$ *in the case* $\beta < 1$. *As* λ *increases, with other parameters fixed, the convergence order decreases, aligning with Theorem 3.2. The numerical results in Table 4 and Figure 3 validate these theoretical findings.*

Table 4. Maximum errors and convergence orders for the fractional Adams-Simpson-type scheme (2.5) applied to Example 3 with $\beta = 0.6$.

λ	N	$\alpha = 0.1$		$\alpha = 0.2$		$\alpha = 0.3$	
		E(N)	O(N)	E(N)	O(N)	E(N)	O(N)
2.5	2^4	3.9054e-02	1.41	4.7580e-02	1.39	6.8513e-02	1.33
	2^5	1.4697e-02	1.85	1.8118e-02	1.99	2.7267e-02	2.13
	2^6	4.0888e-03	2.29	4.5511e-03	3.53	6.2454e-03	3.46
	2^7	8.3324e-04	–	3.9388e-04	–	5.6633e-04	–
3	2^4	4.2525e-02	1.25	5.1407e-02	1.24	7.3678e-02	1.20
	2^5	1.7875e-02	1.74	2.1810e-02	1.85	3.1978e-02	1.97
	2^6	5.3356e-03	2.18	6.0333e-03	3.02	8.1878e-03	4.48
	2^7	1.1809e-03	–	7.4525e-04	–	3.6656e-04	–
4	2^4	4.6008e-02	0.95	5.5223e-02	0.94	7.8650e-02	0.94
	2^5	2.3791e-02	1.56	2.8699e-02	1.62	4.0953e-02	1.69
	2^6	8.0840e-03	2.00	9.3407e-03	2.44	1.2694e-02	3.46
	2^7	2.0251e-03	–	1.7172e-03	–	1.1541e-03	–

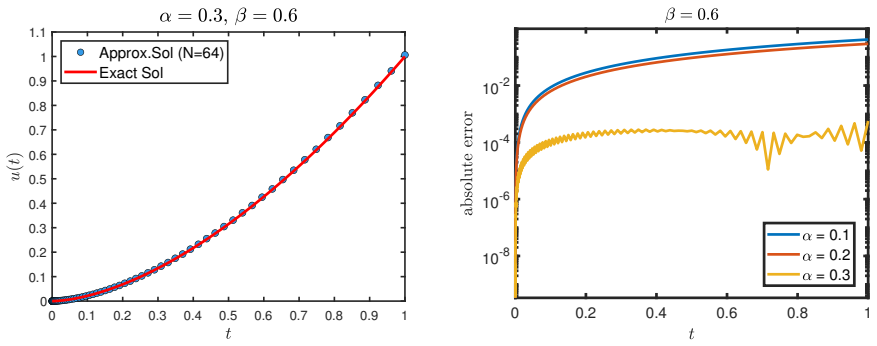

(a) (b)

Figure 3. Graphs of $u(t)$ and the absolute error for Example 3 with $\beta = 0.6$. (a) The contrast of the exact solution (red curve) against discrete numerical approximations (blue markers) with $\lambda = 2.5$. (b) The absolute error at each node under different α values and $\lambda = 2.5$.

Figure 3 compares the exact solution $u(t)$ with numerical approximations and displays the absolute errors, which illustrate the precision of the numerical method and demonstrate the impact of different values of α on the error.

The three numerical experiments demonstrate the robustness of the fractional Adams-Simpson-type algorithm for VIE3 (1.1) across different cases, namely $\beta = 1$, $\beta > 1$, and $\beta < 1$, with varying parameters of $K(t, s)$, α, λ and distinct exact solutions. In all cases, the observed convergence order gradually approaches the theoretical convergence order as the step size decreases, confirming the effectiveness of the scheme for solving VIE3. The consistent agreement between the numerical results and Theorem 3.2 further underscores the reliability of the proposed method. From Figures 1–3, one can observe that for slightly larger α, the absolute errors exhibit more oscillations across the nodes but are overall smaller in magnitude. The smaller error level is expected since a larger α corresponds to a weaker kernel singularity and thus a smoother solution, leading to higher numerical accuracy. The oscillations arise from the non-uniform distribution of the grid nodes: The graded mesh is highly refined near $t = 0$ to resolve the initial singularity and becomes coarser as t increases, causing the error distribution to fluctuate. This behavior is fully consistent with the theoretical stability result in Theorem 3.3, which guarantees that the numerical scheme remains stable for all $\alpha \in [0, 1)$.

5. Conclusions

In this work, a fractional Adams-Simpson-type numerical scheme with non-uniform grid strategy is established to solve VIE3. A modified fractional Grönwall inequality is employed to rigorously analyze the stability and convergence of the algorithm. Theoretical analysis shows that the algorithm can achieve the optimal convergence order $4 - \alpha - \lambda\beta$ when the grid parameter $\lambda = (4 - \alpha) / (\sigma + 1 - \alpha)$. Numerical experiments validate the theoretical conclusions and confirm the computational precision of the proposed scheme in handling VIE3. An interesting direction for future research is the extension of the proposed method to VIE3 with variable-exponent weakly singular kernels, where the exponent $\alpha = \alpha(t)$ depends on time. The non-uniform grid strategy and high-order

interpolation framework developed in this paper may provide a useful foundation for such an extension. More broadly, modern scientific machine learning approaches such as physics-informed neural networks (PINNs) and neural operators have been rapidly developed for solving VIEs. While these methods offer mesh-free flexibility and can handle high-dimensional problems, they often lack rigorous error guarantees when solutions exhibit initial singularities. In contrast, the proposed method provides provable convergence rates even for non-smooth solutions. Furthermore, the graded mesh theory developed here may offer useful guidance for designing adaptive sampling or collocation strategies in neural network-based solvers for singular integral equations.

Use of AI tools declaration

The authors declare they have not used Artificial Intelligence (AI) tools in the creation of this article.

Acknowledgments

This work is supported by the Northeast Forestry University College Student Innovation and Entrepreneurship Training Program Project (Grant Number: DCLXY-202608) and the Natural Science Foundation of Heilongjiang Province of China (Grant Number: PL2024A002).

Conflict of interest

The authors declare there are no conflicts of interest.

References

1. S. S. Allaei, Z. W. Yang, H. Brunner, Existence, uniqueness and regularity of solutions to a class of third-kind Volterra integral equations, *J. Integral Equ. Appl.*, **27** (2015), 325–342. https://doi.org/10.1216/JIE-2015-27-3-325
2. G. Vainikko, Cordial Volterra integral equations 1, *Numer. Funct. Anal. Optim.*, **30** (2009), 1145–1172. https://doi.org/10.1080/01630560903393188
3. G. Vainikko, Cordial Volterra integral equations 2, *Numer. Funct. Anal. Optim.*, **31** (2010), 191–219. https://doi.org/10.1080/01630561003666234
4. H. Chen, J. Ma, Solving the third-kind Volterra integral equation via the boundary value technique: Lagrange polynomial versus fractional interpolation, *Appl. Math. Comput.*, **414** (2022), 126685. https://doi.org/10.1016/j.amc.2021.126685
5. C. Lubich, Fractional linear multistep methods for Abel-Volterra integral equations of the second kind, *Math. Comp.*, **45** (1985), 463–469. https://doi.org/10.1090/S0025-5718-1985-0804935-7
6. C. Lubich, Discretized fractional calculus, *SIAM J. Math. Anal.*, **17** (1986), 704–719. https://doi.org/10.1137/0517050
7. R. Lin, F. Liu, Fractional high order methods for the nonlinear fractional ordinary differential equation, *Nonlinear Anal. Theory Methods Appl.*, **66** (2007), 856–869. https://doi.org/10.1016/j.na.2005.12.027

8. K. Diethelm, N. J. Ford, A. D. Freed, A predictor-corrector approach for the numerical solution of fractional differential equations, *Nonlinear Dyn.*, **29** (2002), 3–22. https://doi.org/10.1023/A:1016592219341

9. K. Diethelm, N. J. Ford, A. D. Freed, Detailed error analysis for a fractional Adams method, *Numer. Algorithms*, **36** (2004), 31–52. https://doi.org/10.1023/B:NUMA.0000027736.85078.be

10. C. Li, C. Tao, On the fractional Adams method, *Comput. Math. Appl.*, **58** (2009), 1573–1588. https://doi.org/10.1016/j.camwa.2009.07.050

11. Y. Yan, K. Pal, N. J. Ford, Higher order numerical methods for solving fractional differential equations, *BIT Numer. Math.*, **54** (2014), 555–584. https://doi.org/10.1007/s10543-013-0443-3

12. Y. Liu, J. Roberts, Y. Yan, A note on finite difference methods for nonlinear fractional differential equations with non-uniform meshes, *Int. J. Comput. Math.*, **95** (2018), 1151–1169. https://doi.org/10.1080/00207160.2017.1381691

13. Y. Liu, J. Roberts, Y. Yan, Detailed error analysis for a fractional Adams method with graded meshes, *Numer. Algorithms*, **78** (2018), 1195–1216. https://doi.org/10.1007/s11075-017-0419-5

14. P. Lyu, S. Vong, A high-order method with a temporal nonuniform mesh for a time-fractional Benjamin–Bona–Mahony equation, *J. Sci. Comput.*, **80** (2019), 1607–1628. https://doi.org/10.1007/s10915-019-00991-6

15. X. Zheng, Two methods addressing variable-exponent fractional initial and boundary value problems and Abel integral equation, *CSIAM Trans. Appl. Math.*, **6** (2025), 666–710. https://doi.org/10.4208/csiam-am.SO-2024-0052

16. H. Brunner, On the divergence of collocation solutions in smooth piecewise polynomial spaces for Volterra integral equations, *BIT Numer. Math.*, **44** (2004), 631–650. https://doi.org/10.1007/s10543-004-3828-5

17. Y. M. Wang, B. Xie, A fractional Adams–Simpson-type method for nonlinear fractional ordinary differential equations with non-smooth data, *BIT Numer. Math.*, **63** (2023), 7. https://doi.org/10.1007/s10543-023-00952-4

18. B. Li, S. Ma, A high-order exponential integrator for nonlinear parabolic equations with nonsmooth initial data, *J. Sci. Comput.*, **87** (2021), 23. https://doi.org/10.1007/s10915-021-01438-7

19. B. Li, S. Ma, Exponential convolution quadrature for nonlinear subdiffusion equations with nonsmooth initial data, *SIAM J. Numer. Anal.*, **60** (2022), 503–528. https://doi.org/10.1137/21M1421386

20. H. L. Liao, D. Li, J. Zhang, Sharp error estimate of the nonuniform L1 formula for linear reaction-subdiffusion equations, *SIAM J. Numer. Anal.*, **56** (2018), 1112–1133. https://doi.org/10.1137/17M1131829

21. M. Stynes, E. O'Riordan, J. L. Gracia, Error analysis of a finite difference method on graded meshes for a time-fractional diffusion equation, *SIAM J. Numer. Anal.*, **55** (2017), 1057–1079. https://doi.org/10.1137/16M1082329

22. C. Li, Q. Yi, A. Chen, Finite difference methods with non-uniform meshes for nonlinear fractional differential equations, *J. Comput. Phys.*, **316** (2016), 614–631. https://doi.org/10.1016/j.jcp.2016.04.039

23. D. Baleanu, *Fractional Calculus: Models and Numerical Methods*, World Scientific, 2012.

AIMS Press